

Nanoscale

Accepted Manuscript



This is an *Accepted Manuscript*, which has been through the Royal Society of Chemistry peer review process and has been accepted for publication.

Accepted Manuscripts are published online shortly after acceptance, before technical editing, formatting and proof reading. Using this free service, authors can make their results available to the community, in citable form, before we publish the edited article. We will replace this *Accepted Manuscript* with the edited and formatted *Advance Article* as soon as it is available.

You can find more information about *Accepted Manuscripts* in the [Information for Authors](#).

Please note that technical editing may introduce minor changes to the text and/or graphics, which may alter content. The journal's standard [Terms & Conditions](#) and the [Ethical guidelines](#) still apply. In no event shall the Royal Society of Chemistry be held responsible for any errors or omissions in this *Accepted Manuscript* or any consequences arising from the use of any information it contains.

ARTICLE

Self-carried Curcumin Nanoparticles for *In vitro* and *In vivo* Cancer Therapy with Real-time Monitoring of Drug Release

Cite this: DOI: 10.1039/x0xx00000x

Jinfeng Zhang^{a,d†}, Shengliang Li^{b†}, Fei-Fei An^a, Juan Liu^b, Shubin Jin^b, Jin-Chao Zhang^c, Paul C. Wang^f, Xiaohong Zhang^{a,c*}, Chun-Sing Lee^{d*}, and Xing-Jie Liang^{b*}Received xxxx 2015,
Accepted xxxx 2015

DOI: 10.1039/x0xx00000x

www.rsc.org/Nanoscale

The use of different nanocarriers for delivering hydrophobic pharmaceutical agents to tumor sites has garnered major attention. Despite the merits of these nanocarriers, further studies are needed for improving their drug loading capacities (typically less than 10%) and reducing their potential systemic toxicity. So development of alternative self-carried nanodrug delivery strategies without using any inert carriers is highly desirable. In this study, we developed a self-carried curcumin (Cur) nanodrug for highly effective cancer therapy *in vitro* and *in vivo* with real-time monitoring of drug release. With a biocompatible C₁₈PMH-PEG functionalization, the Cur nanoparticles (NPs) showed excellent dispersibility and outstanding stability in physiological environment, with drug loading capacity higher than 78 wt.%. Both confocal microscopy and flow cytometry confirmed the cellular fluorescent “OFF-ON” activation and real-time monitoring of Cur molecule release. *In vitro* and *in vivo* experiments clearly show that therapeutic efficacy of the PEGylated Cur NPs is much better than that of free Cur. This self-carried strategy with real-time monitoring of drug release may open a new way for simultaneous cancer therapy and monitoring.

1. Introduction

Cancer challenges the survival of people in the world and accounts for several millions of deaths every year.^{1,2} Among various treatments against cancer, chemotherapy is a dominant modality for its high efficiency comparing with other treatments. Unfortunately, most conventional anticancer drugs are hydrophobic and have no specific selectivity; these thus lead to various problems including poor bioavailability, rapid blood/renal clearance, low accumulation in tumors, and adverse side effects for healthy tissues.³⁻⁹ To overcome these drawbacks, much current attention has been drawn to the use of nanostructured carriers for encapsulating active drug molecules. This approach can effectively deliver hydrophobic anticancer drugs to tumor sites with improved therapeutic activity and reduced side effects.¹⁰⁻¹⁶ However, as most nanocarriers reported are inert in human body and have no therapeutic efficacy by themselves, their applications raises concerns regarding their possible toxicities and the biodegradation. Furthermore, drug loading capacity of such nanocarrier-based drug delivery system (DDS) is comparatively low (typically less than 10%) and this would reduce the effective tumor accumulation and therapeutic efficacy of the anticancer drugs.¹⁷⁻²⁰ Therefore, development of alternative self-carried nanodrug delivery strategies without using any inert carriers is highly desirable.²¹⁻²⁶ In 2012, Kasai *et al.* modified the drug-solvent interactions by jointing two drug molecules into a dimer

which enable them to form self-carried pure nanodrugs of 30-50 nm sizes via reprecipitation method.²² Recently, our group has developed an AAO-template-assisted approach for preparing 20 to 100 nm sized self-carried nanodrugs with good size and morphological controls.²⁶ However, so far most reported self-carried nanodrugs give no or weak fluorescence and thus do not provide signal for tracking their releases.

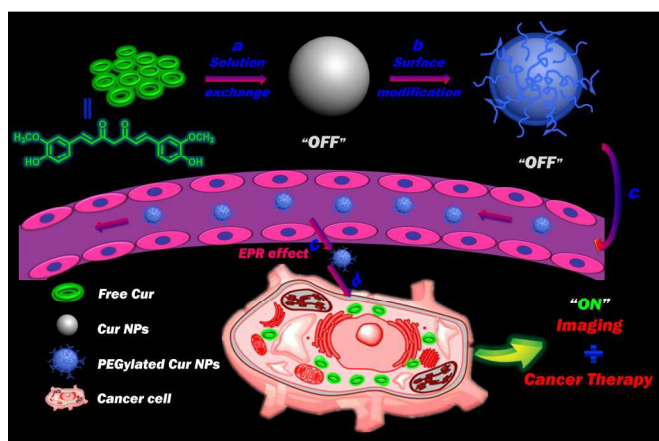
On the other hand, activatable theranostic agents that combines fluorescent and cytotoxic modalities allowing real-time monitoring of drug release in physiological systems has recently gained considerable attention.²⁷⁻³³ As most antitumor drugs give no or weak fluorescence, the most prevalent strategy for getting such theranostic agents is to load drugs into inert fluorescent NPs or trap drugs and fluorescent dyes into non-fluorescent NPs (e.g. coumarin, silicon, carbon etc.).^{12,14,30,34} However, these inert fluorescent NPs or fluorescent dyes lack therapeutic modality which leads to the mentioned issues of low drug loading capacities and potential long-term toxicities of carrier-based DDS. Furthermore, the design and synthesis of such multi-component DDS are usually time-consuming and involve complicated procedures. To address these problems, self-carried nanodrugs have been developed and demonstrate to have superior performance.²¹⁻²⁶ However, so far most reports on self-carried nanodrugs involve only *in vitro* cancer therapy; and there are few reports on their *in vivo* application.^{20,35} While it is thus highly desirable to develop self-carried nanodrug without any redundant fluorophor for *in vitro* and *in vivo* cancer therapy

with real-time monitoring capacity, this is so far not achieved to the best of our knowledge.

Herein, we choose curcumin (Cur), a hydrophobic polyphenol derived from the rhizome of the herb *Curcuma longa*, as a model hydrophobic drug to demonstrate the merits of the strategy. Cur exhibits a wide range of pharmacological effects including anti-inflammatory, anti-cancer, and anti-angiogenic properties to many tumor cell lines.^{36,37} Despite Cur's remarkable anticancer characteristics, its extremely low water solubility and poor bioavailability are impeding its wide clinical use. To address this issue, in previous works, Cur has been loaded into various inert carriers such as mesoporous silica nanoparticles,^{38,39} gold nanoparticles⁴⁰ and polymeric nanoparticles.^{41,42} However, besides their low Cur-loading capacities, the large amount of inert carriers used could lead to other concerns including their metabolisms and potential long-term toxicities.¹⁷⁻²⁰ Another reason for choosing Cur in this study is Cur's different fluorescent characteristics in its solid and molecular forms. While isolated Cur molecule gives strong green fluorescence (ON state), Cur solid shows no emission (OFF state) because of intermolecular aggregation. This two emission states is exploited in this study for monitoring the release of Cur molecules (ON) from drug nanoparticles (OFF) upon cell internalization. In this paper, Cur NPs are first prepared by reprecipitation method and then followed by surface functionalization with poly(maleic anhydride-alt-1-octadecene)-polyethylene glycol (C₁₈PMH-PEG) through hydrophobic interaction to achieve better biocompatibility, which exhibit significantly enhanced drug efficacy to colon carcinoma cells (CT-26 cells) with real-time monitoring of drug release and display improved tumor inhibition in CT-26 cell bearing mice comparing to free Cur drugs.

2. Results and Discussion

2.1 Preparation, characterization and surface functionalization of Self-carried Cur NPs



Scheme 1. Schematic illustration of functionalized self-carried Cur NPs from nanoparticle formation, PEGylation to delivery. (a) Preparation of pure Cur NPs with no fluorescence (OFF) via solution exchange method. Upper-left: the chemical structure of Cur. (b) Surface modification of the pure Cur NPs with C₁₈PMH-PEG through hydrophobic interaction. (c) Passive tumor targeting is achieved via the EPR effect, which facilitates the PEGylated Cur NPs to access tumors by way of their leaky

vasculature. (d) The PEGylated Cur NPs entered tumor cells by endocytosis and released the Cur molecules which recover their strong green fluorescence (ON).

Our proposed strategy for preparing self-carried pure Cur NPs for cancer therapy with real-time monitoring of drug release is illustrated in Scheme 1. The self-carried Cur NPs were prepared by reprecipitation method in which Cur dissolved in tetrahydrofuran (THF) solution was rapidly injected into deionized water under vigorous stirring. Due to the sudden change in solvent environment, Cur molecules will aggregate and precipitate out to form NPs. We choose the well documented reprecipitation approach here is because the technique is very simple but versatile, it is widely employed in many biomedical researches including many recent works.⁴³⁻⁴⁷ Fig. 1a and Fig. S1a show respectively an SEM and a TEM images of the Cur NPs in the form of well-defined and monodispersed nanospheres of 80-90 nm in diameter. Dynamic light scattering measurement (DLS, see Fig. 1b) presents a hydrodynamic diameter of 83.2 nm and a polydispersity index (PDI) value of 0.18.

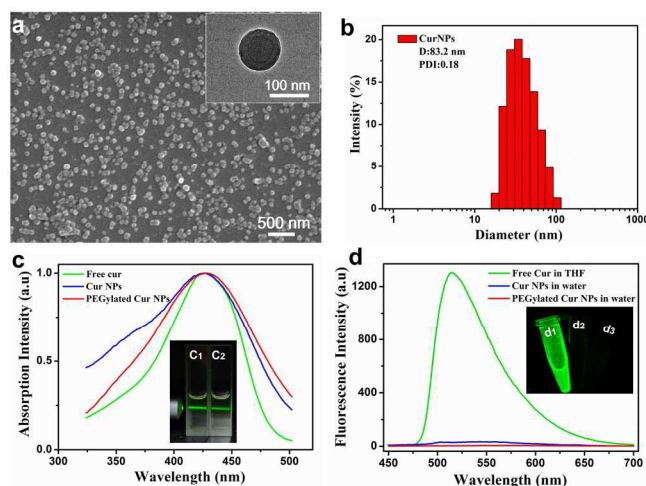


Fig. 1. Characterization and photo-physical properties of Cur NPs. a) an SEM image of the as-prepared Cur NPs (Inset is a corresponding TEM image). b) DLS and PDI measurements of the as-prepared Cur NPs in deionized water. c) Absorption and d) fluorescence spectra of free Cur dissolved in THF, the as-prepared Cur NPs and the PEGylated Cur NPs dispersed in deionized water. Inset in (c) displays that a beam of green laser shines through the samples showing scattering from the NPs via the Tyndall effect (c1: as-prepared Cur NP; c2: the PEGylated Cur NP). Inset in (d) shows photograph of the fluorescence from the three samples (d1: free Cur; d2: as-prepared Cur NP; d3: the PEGylated Cur NP).

To enhance their biocompatibility for facilitating further *in vivo* application, surface modification of the as-prepared Cur NPs is essential. Previous researchers have demonstrated that PEG is an effective biocompatible building block that has been widely applied to biomaterials for reducing nonspecific adsorption of biological substances and provide excellent long-term *in vivo* stability.⁴⁸⁻⁵¹ Here, C₁₈PMH-PEG was anchored to the surface of the as-prepared Cur NPs by ultrasonication (the product hereafter referred as PEGylated Cur NPs). Fig. S1b show a TEM image and a DLS measurement (inset) of the PEGylated Cur NPs with sizes around 100 nm. We also measured zeta potentials of the Cur NPs and the PEGylated Cur

NPs which both displays negative charge (Fig. S2). Fig. S3 presents the digital photographs of different samples including free Cur in THF, free Cur, Cur NPs and PEGylated Cur NPs dispersed in water respectively, which show a good dispersibility and better stability of NP than that of free drug in water. We also observed that while the PEGylated Cur NPs exhibit high stability in water and physiological saline even over 5 days, the as-prepared Cur NPs show fast agglomeration into larger particles (Fig. S4). Thus, it demonstrates that surface functionalization of Cur NPs was successfully achieved with excellent water stability, thus making the PEGylated Cur NPs *in vivo* drug delivery possible.

An obvious advantage of self-carried pure nanodrug delivery systems is their high drug loading capacities. Owing to no addition of any inert excipients, the average Cur loading efficiency and encapsulation efficiency here are estimated to be 78.5% and 95.8% respectively by using standard absorbance technique (Fig. S5). This loading capacity is much higher than those achieved with carrier-based DDS (typically less than 10%) and is the highest value reported among all reported Cur-based nanomedicine (Table S1).

To further investigate photo-physical properties of the Cur NPs, we measured absorption and fluorescence spectra of free Cur dissolved in THF, the as-prepared Cur NPs and the PEGylated Cur NPs dispersed in deionized water. As exhibited in Figure 1c, the three samples show similar absorption spectra with the same Cur characteristic absorption peak at about 428 nm suggesting that the Cur molecular structure remains unchanged in preparation process. As expected, the free Cur solution shows strong green fluorescence (ON), while the two Cur NP dispersions show no fluorescence (OFF) (Fig. 1d) because of aggregation-caused quenching effect. When Cur NPs enter tumor cells, Cur molecule will be released and recovering its green fluorescence again (ON). Subsequent cell imaging experiments will further confirm the successful implementation of this fluorescent “OFF-ON” system which enables self-monitoring of Cur drug release.

2.2 Cumulative drug release profiles

The drug release profile is of great importance for practical drug delivery applications of the proposed DDS. Concentrations of released Cur were determined via absorption measurement (Fig. S5). As depicted in Fig. 2, in the first 32 hours, the as-prepared Cur NPs reached approximately 46 wt% drug release and the PEGylated Cur NPs exhibited about 36 wt% drug release. Due to dissolution of the exterior PEG layer, the PEGylated Cur NPs show a slower release comparing to the as-prepared Cur NPs. Both of these two as-prepared NPs show no initial burst release, but a sustained release feature with over 60%, and Cur being released for as long as 300 hours. The slow and steady release without burst discharge of the Cur NPs is essential for their *in vivo* applications for improved long-term blood circulation and more efficient delivery to tumors with reduced drug leakage on their ways

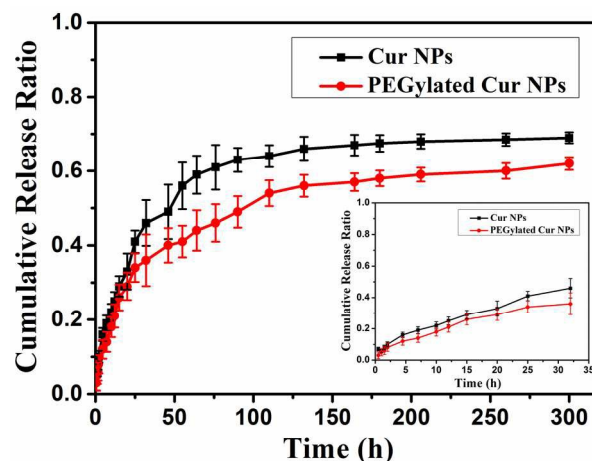


Fig. 2. Cumulative drug releases from the as-prepared Cur NPs and the PEGylated Cur NPs as a function of release time in PBS medium over 300 hours. Inset is the results for the first 32 hours.

2.3 Cellular uptake and imaging of PEGylated Cur NPs

To investigate the cellular uptake and intracellular distribution of the released Cur molecules, the CT-26 cells were incubated with PEGylated Cur NPs at 37 °C for 4 h. Fluorescence images of the incubated cells were taken with a confocal laser scanning microscope, where 4, 6-diamidino-2-phenylindole (DAPI) was used as a nucleus located dye. LysoTracker Red or MitoTracker Red was also used for staining the lysosomes and the mitochondria respectively. As shown in Fig. 3, the intense homogeneous cytoplasmic green fluorescences around the nuclei confirm Cur molecules have been released in the cells. Besides labeling the lysosomal vesicles, the Cur molecules are also able to stain almost everywhere else in the cytoplasm, providing insights into the sub-cellular distribution of the Cur NPs.

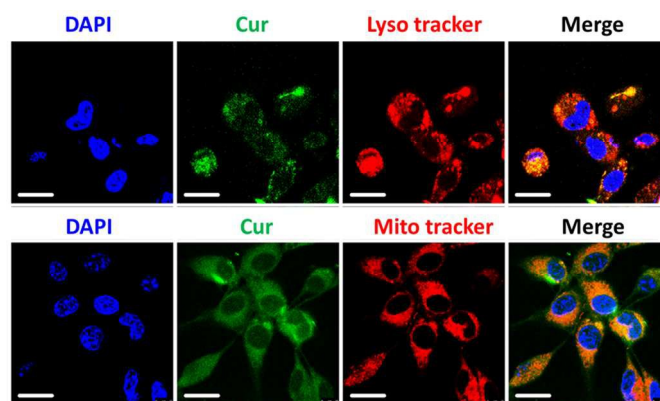


Fig. 3. Confocal microscopic images of colocalized experiment in CT-26 cells. Cell nuclei is stained with DAPI (blue signal) and lysosome and mitochondria are stained with LysoTracker Red (red signal) and Mitotracker Red (red signal) respectively. The upper and lower roles of micrographs show that the Cur molecules have been released into lysosome and mitochondria respectively. Scale bar is 20 μm .

We next studied the cellular fluorescent “OFF-ON” and real-time monitoring of Cur molecule release. The CT-26 cells were cultured with PEGylated Cur NPs for different durations (0,

0.5, 1 and 4 h), and fluorescence from the cells was then analyzed with both confocal microscopy and flow cytometry. As mentioned above, the fluorescence of Cur are quenched (OFF) in the form of NPs, but recovered (ON) upon cell internalization as free molecules. As expected, Fig. 4 and Fig. S6 show that after 30 min or longer incubation duration, green Cur molecular fluorescence (ON) can be detected; whereas no signal (OFF) can be observed at the beginning of incubation since Cur is still in the state of NP. This demonstrates that the present Cur NPs are promising for monitoring drug release with a cellular fluorescent “OFF-ON” action. To further confirm the real-time monitoring capacity of the NPs, flow cytometric analyses of the CT-26 cells after incubation with PEGylated Cur NPs for different durations was shown in Figure S7. Enhanced green fluorescence in the cell was observed after 1 and 4 h of incubations, which could be attributed to Cur molecules gradually released from the NPs in a cellular environment. These results indicated that PEGylated Cur NPs possessed a time-dependent cellular release ability.

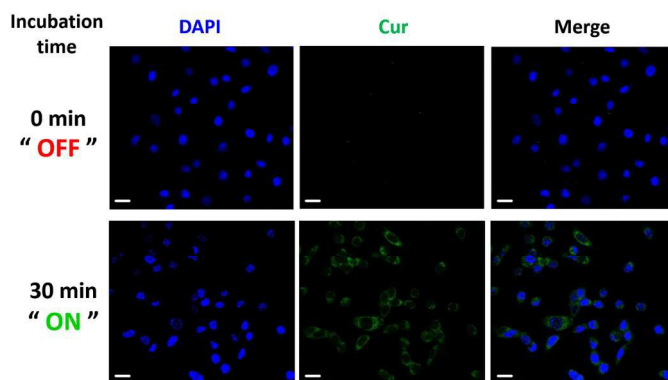


Fig. 4. Confocal microscopic images of the CT-26 cells treated with the PEGylated Cur NPs. The images were taken immediately (upper roll) and 30 min (lower roll) after adding 5 μM of the Cur NPs to the cells. Scale bar is 20 μm .

2.4 *In vitro* cytotoxic activity

We next studied cytotoxicity profiles of the PEGylated Cur NPs to the CT-26 cells compared with free Cur with a MTT assay. As depicted in Fig. 5 and Fig. S8, PEGylated Cur NPs show considerably higher cytotoxicity than the free Cur in all doses. The MTT data reveal that the Cur NPs can obviously inhibit the proliferation of the CT-26 cells, as shown by a 8-fold decrease in the half-maximal inhibitory concentration (IC_{50}) values from the free Cur ($\text{IC}_{50} = 33.4 \mu\text{M}$) to the PEGylated Cur NPs ($\text{IC}_{50} = 4.2 \mu\text{M}$) at 24 h. The improved drug efficiency may be due to the more efficient internalization of the functionalized NPs compared with that of free molecules. To check that the observed cytotoxicity is not caused by the PEG coating, MTT assay was carried out for the $\text{C}_{18}\text{PMH-PEG}$ surfactant. The results as presented in Fig. S9 confirm that the surfactant has no cytotoxicity. Moreover, bright field microscopic images of the CT-26 cells were collected to monitor cell viability directly (Fig. S10). Significant damage to the impregnated CT-26 cells could be clearly observed with the least live cells in the PEGylated Cur NPs incubated group while the control and $\text{C}_{18}\text{PMH-PEG}$ group show no cytotoxicity, which agree well with the MTT experiments. These results show that the self-carried functionalized Cur NPs have improved inhibiting effect on CT-26 cell growth.

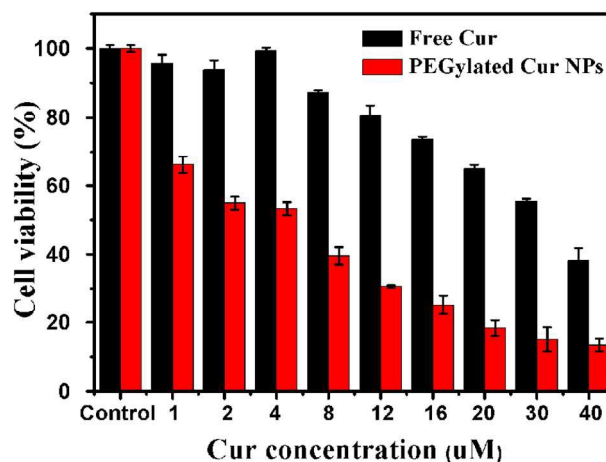


Fig. 5. Cell viability of free Cur and PEGylated Cur NPs in CT-26 cell line after 24 hours of incubation.

2.5 *In vivo* cytotoxic activity

Before intravenous injection, hemolysis assay was performed to confirm the biocompatibility of the PEGylated Cur NPs (Fig. S11). The hemolysis percentages of mice erythrocytes incubated for 3 h at 37 $^{\circ}\text{C}$ with the NPs of different concentrations were determined to be insignificant. This confirms that the PEGylated Cur NPs do not cause erythrocytes rupture. To evaluate whether the PEGylated Cur NPs do have better therapeutic efficacy *in vivo*, CT-26 tumor-bearing nude mice were intravenously injected with free Cur and the PEGylated Cur NPs respectively. For comparison, physiological saline was used as a control for the intravenous injection. Tumor volume and body weight of the tumor-bearing mice were monitored for 21 days. At the end of the experiments, the tumor volumes (Fig. 6a) in mice treated with PEGylated Cur NPs were much smaller than those treated with saline and free Cur. After treatment for 21 days, the tumor volumes in the PEGylated Cur NPs group and the free Cur group are only 32% and 87% respectively of that in the saline group. This shows that the PEGylated Cur NPs do have predominant tumor growth inhibitory efficacy comparing to saline and free Cur. These observations are in accordance with the results of *in vitro* evaluations. In addition, no significant weight loss was observed in the tumor-bearing mice treated with various formulations, indicating negligible side effect of Cur NPs for tumor therapy at the employed dose (10 mg kg^{-1} Cur-equivalent) (Fig. 6b). After treatment for 21 days, the mice were sacrificed and the tumors were dissected and photographed (Fig. 6e). The tumor inhibitory rate (TIR) was calculated from tumor weights (Fig. 6c). Comparing with that of the saline group, TIR of the PEGylated Cur NPs reaches up to 45%, which is significantly higher than that of free Cur (5%) (Fig. 7d). All these results confirm that therapeutic efficacy of the PEGylated Cur NPs is much better than that of the free Cur both *in vitro* and *in vivo*.

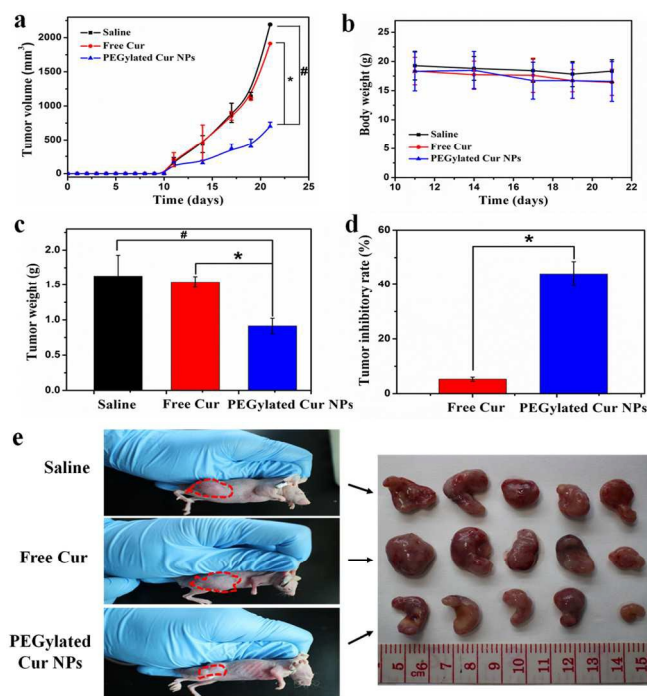


Fig. 6. *In vivo* anticancer activity. a) Tumor volume after intravenous injection of saline, free Cur and PEGylated Cur NPs in CT-26 tumor-bearing nude mice. b) Body weights of CT-26 tumor-bearing mice after treatment with saline, free Cur and PEGylated Cur NPs. c) Mean weight of tumors separated from mice after different treatments. d) The tumor inhibitory rate (TIR) after treatment with free Cur and PEGylated Cur NPs in CT-26 tumor-bearing nude mice. The TIR is calculated using the following equation: $TIR(\%) = 100 \times (\text{mean tumor weight of control group} - \text{mean tumor weight of experimental group}) / \text{mean tumor weight of control group}$. Data are represented as average \pm standard deviation ($n = 5$). Statistical significance: * $P < 0.005$; # $P < 0.001$. (e) The tumor size is real-time monitored during the 21-day evaluation period (Left) and representative tumors separated from animals after intravenous injection of saline, free Cur and PEGylated Cur NPs (Right).

2.6 *In vivo* systematic toxicity

The potential *in vivo* toxicity has always been a great concern in the development of nanomedicines. Besides measuring body weights of mice in each cohort (Fig. 6b), immunohistochemical analysis was also adopted to assess the *in vivo* systematic toxicity of the treatments. Age-matched healthy mice were used as a control group. Standard heart function markers including creatine kinase (CK), aspartate aminotransferase (AST) and lactic dehydrogenase (LDH), liver function markers including alanine aminotransferase (ALT), albumin/globulin ratio (A/G) and total protein (TP), kidney function marker including creatinine (Cr), blood urea nitrogen (BUN) and uric acid (UA) were detected and compared to control (Fig. 7a). No observable toxicity was noted, suggesting no obvious heart, liver and kidney dysfunction of mice induced by the PEGylated Cur NPs treatment. In addition to the blood tests, we collected the main organs of the mice from the control and treated groups and sliced them for hematoxylin and eosin (H&E) staining (Fig. 7b). Neither noticeable organ damage nor inflammation lesion was observed compared with the control group. All these

results evidenced that the PEGylated Cur NPs based *in vivo* cancer treatment induced no significant side effect to the treated mice.

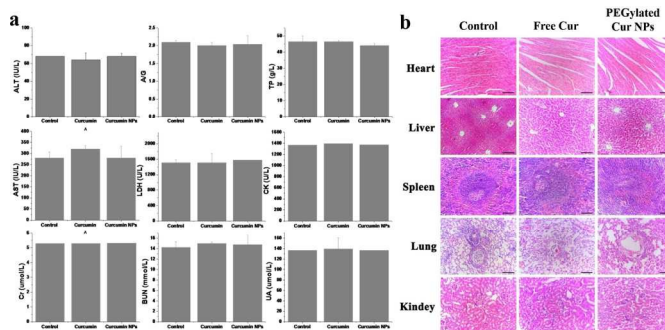


Fig. 7. *In vivo* toxicology study and serum biochemistry results obtained from CT-26-bearing nude mice after intravenous injection with free Cur and PEGylated Cur NPs. a) Blood analysis data of the CT-26-bearing nude mice treated with different formulations after 21 days. Age-matched healthy mice were used as the control group. Data are the mean \pm standard deviation from five separate experiments. b) Hematoxylin and eosin (H&E) stained organ slices from the CT-26-bearing nude mice treated with different formulations after 21 days. Age-matched healthy mice were used as the control group.

3. Conclusions

In summary, we prepared self-carried Cur nanodrugs for highly effective cancer therapy *in vitro* and *in vivo* with real-time monitoring of drug release. With a biocompatible C_{18} PMH-PEG functionalization, the Cur NPs show excellent dispersibility and outstanding stability in physiological environment, with high drug loading capacity higher than 78%. Furthermore, the cellular fluorescent “OFF-ON” activation and real-time monitoring of Cur molecule release were confirmed by both confocal microscopy and flow cytometry, indicating the potential for cancer diagnosis. Finally, both *in vitro* and *in vivo* data clearly show that therapeutic efficacy of the PEGylated Cur NPs is much better than that of free Cur. Above all, the NPs show no observable systematic toxicity *in vivo*. We believe that this self-carried strategy with real-time monitoring of drug release may open a new way for simultaneous cancer therapy and diagnosis.

4. Experimental

4.1 Materials

Curcumin (Cur), poly(maleic anhydride-alt-1-octadecene) (C_{18} PMH), poly(ethylene glycol)-amine (mPEG-NH₂, 5k) and 1-Ethyl-3-(3-dimethylaminopropyl)-carbodiimide (EDC) were purchased from Sigma Aldrich. 3-(4,5-Dimethylthiazol-2-yl)-2,5-diphenyl tetrazolium bromide (MTT) was obtained from Sigma-Aldrich and used after drying in vacuo for 24 h. RPMI 1640 culture medium, fetal bovine serum (FBS), Dulbecco's phosphate buffered saline (PBS), trypsin-EDTA (0.5% trypsin, 5.3mM EDTA tetra-sodium), and the antibiotic agents penicillin-streptomycin (100 U/ml) were from Invitrogen (USA). High-purity water with a resistivity greater than 18.4 M Ω -cm was collected from an in-line Millipore RiOs/Origin water purification system. Unless otherwise noted, all

chemicals were used without further purification. C₁₈PMH-PEG was synthesized following the literature procedure.^{52,53} Briefly, 10 mg (1 eq) of C₁₈PMH and 143 mg (1 eq) of mPEG-NH₂ were dissolved in 5 mL of dichloromethane, 6 μ L triethylamine and 10 mg of EDC. After 24 h of stirring, the solvents were evaporated by blowing with dry N₂. The leftover solid was dissolved in water, forming a transparent clear solution, which was dialyzed against distilled water for 3 days in a dialysis bag with molecular weight cut-off of 14000 Da to remove unreacted mPEG-NH₂. After lyophilization, the final product in a white solid was stored at 4 °C for future use.

4.2 Preparation and functionalization of self-carried Cur NPs

In a typical run, 1.5 mM of Cur was first dissolved in tetrahydrofuran (THF). 200 μ L of the solution was then quickly injected into 5 mL of high-purity water under vigorous stirring at room temperature. For functionalization of the Cur NPs, 300 μ L of C₁₈PMH-PEG (0.9 mg) aqueous solution was added to 5 mL of the Cur NPs suspensions, and sonicated for 5 min. Through this process, C₁₈PMH-PEG would attach to the surface of the Cur NPs by noncovalent hydrophobic interaction.

Drug loading capacity (DLC) and drug loading efficiency (DLE) were calculated according to the following formulae: DLC (wt. %) = (weight of loaded drug/weight of PEGylated Cur NPs) \times 100%; DLE (%) = (weight of loaded drug/weight of drug in feed) \times 100%. The weight of loaded drug and weight of drug in feed was determined with the UV-Vis absorption spectra at 428 nm and calculated by using standard absorbance technique (Fig. S5). The weight of PEGylated Cur NPs was calculated by electronic balance after freeze-drying.

4.3 Characterization of Cur and PEGylated Cur NPs

Sizes and morphologies of the Cur and the PEGylated Cur NPs were examined with SEM (HITACHI S-4300) and TEM (JEM-2100). SEM samples were prepared by drying the nanoparticles onto a Si substrate followed by a 2 nm layer of Au coating. Hydrodynamic sizes of the NPs were measured in aqueous solutions using a DLS instrument (Malvern Zetasizer Nano ZS). Ultraviolet-visible (UV-vis) and fluorescence spectra were respectively recorded with a Hitachi U-3900 and a Hitachi F-4600 systems.

4.4 *In vitro* drug-release

Firstly, Cur NPs, PEGylated Cur NPs were diluted by PBS at pH 7.4. Secondly, five milliliters of each suspension were added into a dialysis bag (3500 molecular weight cut-off, Fisherbrand®, Pittsburgh, PA, USA) followed by immersion in 200 ml of PBS at 37 °C with constant shaking. Thirdly, aliquots of 2 ml were collected from the solution at certain time points. During the dialysis, the solution volume was maintained constant by topping up 2 ml of PBS after each sampling. The amount of the released Cur was measured by UV-Vis absorbance. The assay was performed 3 times for each sample.

4.4 Cell culture

CT-26 cells were cultured with RPMI 1640 (Invitrogen, USA) supplemented with 10 % FBS (Hyclone Company, South Logan, UT), penicillin (100 μ g/mL), and streptomycin (100 μ g/mL; Gibco, Grand Island, NY, USA) in 5% CO₂ at 37 °C in a humidified incubator.

4.5 Confocal laser scanning microscopy

Imaging of cells was performed using a Leica laser scanning confocal microscope. CT-26 cells were seeded in a 24-well cell-culture plate for 24 h (37 °C, 5% CO₂). Then PEGylated Cur NPs were added to the wells. The cells were then incubated for 30 min, 1h and 4 h (37 °C, 5% CO₂). Before observation, the cells were washed three times with PBS and then fixed with 4% paraformaldehyde. Imaging was performed under 488 nm laser excitation and the emission was collected within the range of 515-550 nm. The control group was the cells without incubation with the NPs.

4.6 *In vitro* cytotoxicity

Cell cytotoxicity was determined through a standard MTT assay. CT-26 cells were seeded into a 96-well cell-culture plate with 100 μ L (5000 cells) per well at and then incubated for 24 h at 37°C under 5% CO₂. Then the cells were incubated with free Cur, PEGylated Cur NPs of different concentrations for 24h and 48h respectively before the MTT assay.

4.7 *In vivo* antitumor efficacy

Female BALB/c nude mice of 18-20 g were purchased from Vital River Company (Beijing, China) and raised under standard pathogen-free conditions. All animal experiments were performed in accordance with the principles of care and use of laboratory animals. The tumor xenografts were implanted in the BALB/c nude mice by injecting 3 \times 10⁶ CT-26 cells into the right flank of each mouse. The xenografted mice were randomly divided into 3 groups (five mice per group) when the tumor volume reached about 100 mm³. Saline, free Cur, PEGylated Cur NPs were administered by intravenous (i.v.) injection at a Cur-equivalent dose of 10 mg/kg every 3 days. Tumor progression in the mice was then monitored every three days. The mice were sacrificed and their tumors were immediately removed and weighed. Meanwhile, plasma was collected for biochemical studies, including assays for respectively heart, liver and renal functions. Haematoxylin/eosin (H&E) staining of the tumor sections were carried out for tissues studies.

4.8 Statistical Analysis

All data are presented as means \pm standard deviation (S.D.). The significant differences between groups were evaluated with the Tukey's method after analysis of variance (ANOVA). In all statistical analyses, $p < 0.05$ was considered to be statistically significant.

Acknowledgements

This work was supported by the Chinese Natural Science Foundation general project (81171455) and key project (31430031), National Distinguished Young Scholars grant (31225009) from the National Natural Science Foundation of China, National Key Basic Research Program of China (2009CB930200), Chinese Academy of Sciences (CAS) "Hundred Talents Program" (07165111ZX), CAS Knowledge Innovation Program and State High-Tech Development Plan (2012AA020804 and SS2014AA020708), and the Key Basic Research Special Foundation of Science Technology Ministry of Hebei Province (Grant No. 14961302D). This work was also supported in part by NIH/NIMHD 8 G12 MD007597, and

USAMRMC W81XWH-10-1-0767 grants. The authors also appreciate the support by the "Strategic Priority Research Program" of the Chinese Academy of Sciences, Grant No. XDA09030301 and support by the external cooperation program of BIC, Chinese Academy of Science, Grant No. 121D11KYSB20130006.

Notes and references

a Nano-organic Photoelectronic Laboratory, Technical Institute of Physics and Chemistry, Chinese Academy of Sciences, 100190 Beijing, P. R. China.

b Chinese Academy of Sciences (CAS) Key Laboratory for Biological Effects of Nanomaterials and Nanosafety, National Center for Nanoscience and Technology, Beijing, P. R. China.

c Functional Nano & Soft Materials Laboratory (FUNSOM) and Jiangsu Key Laboratory for Carbon-Based Functional Materials & Devices, Soochow University, Suzhou, P. R. China.

d Center of Super-Diamond and Advanced Films (COSDAF) & Department of Physics and Materials Science, City University of Hong Kong, Hong Kong SAR, P. R. China.

e College of Chemistry & Environmental Science, Chemical Biology Key Laboratory of Hebei Province, Hebei University, Baoding, P. R. China.

f Molecular Imaging Laboratory, Department of Radiology, Howard University, Washington D.C., USA.

† These authors contributed equally to this work.

* Corresponding author.

E-mail: xiaohong_zhang@suda.edu.cn

E-mail: apcslee@cityu.edu.hk

E-mail: liangxj@nanocr.cn

Electronic Supplementary Information (ESI) available: [details of any supplementary information available should be included here]. See DOI: 10.1039/b000000x/

- 1 D. Peer, J. M. Karp, S. Hong, O. C. Farokhzad, R. Margalit, R. Langer, *Nat. Nanotechnol.* 2007, **2**, 751.
- 2 R. Siegel, D. Naishadham, A. Jemal, *CA Cancer J. Clin.* 2013, **63**, 11.
- 3 J. H. Atkins, L. J. Gershell, *Nat. Rev. Cancer* 2002, **2**, 645.
- 4 B. A. Chabner, T. G. Roberts, *Nat. Rev. Cancer* 2005, **5**, 65.
- 5 D. J. Irvine, *Nat. Mater.* 2011, **10**, 342.
- 6 J. A. Hubbell, R. Langer, *Nat. Mater.* 2013, **12**, 963.
- 7 S. Mura, J. Nicolas, P. Couvreur, *Nat. Mater.* 2013, **12**, 991.
- 8 G. Cafeo, G. Carbotti, A. Cuzzola, M. Fabbri, S. Ferrini, F. H. Kohnke, G. Papanikolaou, M. R. Plutino, C. Rosano, A. J. P. White, *J. Am. Chem. Soc.* 2013, **135**, 2544.
- 9 X. Wu, X. Sun, Z. Guo, J. Tang, Y. Shen, T. D. James, H. Tian, W. Zhu, *J. Am. Chem. Soc.* 2014, **136**, 3579.
- 10 Y. Zhou, W. Huang, J. Liu, X. Zhu, D. Yan, *Adv. Mater.* 2010, **22**, 4567.
- 11 M. N. Holme, I. A. Fedotenko, D. Abegg, J. Althaus, L. Babel, F. Favarger, R. Reiter, R. Tanasescu, P. L. Zaffalon, A. Ziegler, B. Muller, T. Saxer, A. Zumbuehl, *Nat. Nanotechnol.* 2012, **7**, 536.
- 12 M. H. Lee, J. Y. Kim, J. H. Han, S. Bhuniya, J. L. Sessler, C. Kang, J. S. Kim, *J. Am. Chem. Soc.* 2012, **134**, 12668.
- 13 F. Peng, Y. Su, X. Wei, Y. Lu, Y. Zhou, Y. Zhong, S. T. Lee, Y. He, *Angew. Chem. Int. Ed.* 2013, **52**, 1457.
- 14 S. Maiti, N. Park, J. H. Han, H. M. Jeon, J. H. Lee, S. Bhuniya, C. Kang, J. S. Kim, *J. Am. Chem. Soc.* 2013, **135**, 4567.
- 15 Q. Xing, N. Li, D. Chen, W. Sha, Y. Jiao, X. Qi, Q. Xu, J. Lu, *J. Mater. Chem. B* 2014, **2**, 1182.
- 16 P. Zhang, F. Cheng, R. Zhou, J. Cao, J. Li, C. Burda, Q. Min, J. Zhu, *Angew. Chem. Int. Ed.* 2014, **53**, 2371.
- 17 C. A. Poland, R. Duffin, I. Kinloch, A. Maynard, W. A. H. Wallace, A. Seaton, V. Stone, S. Brown, W. MacNee, K. Donaldson, *Nat. Nanotechnol.* 2008, **3**, 423.
- 18 Y. Shen, E. Jin, B. Zhang, C. J. Murphy, M. Sui, J. Zhao, J. Wang, J. Tang, M. Fan, E. V. Kirk, W. J. Murdoch, *J. Am. Chem. Soc.* 2010, **132**, 4259.
- 19 A. M. Alkilany, A. Shatanawi, T. Kurtz, R. B. Caldwell, R. W. Caldwell, *Small* 2012, **8**, 1270.
- 20 P. Huang, D. Wang, Y. Su, W. Huang, Y. Zhou, D. Cui, X. Zhu, D. Yan, *J. Am. Chem. Soc.* 2014, **136**, 11748.
- 21 K. Baba, H. E. Pudavar, I. Roy, T. Y. Ohulchanskyy, Y. Chen, R. K. Pandey, P. N. Prasad, *Mol. Pharm.* 2007, **4**, 289.
- 22 H. Kasai, T. Murakami, Y. Ikuta, Y. Koseki, K. Baba, H. Oikawa, H. Nakanishi, M. Okada, M. Shoji, M. Ueda, H. Imahori, M. Hashida, *Angew. Chem. Int. Ed.* 2012, **51**, 10315.
- 23 W. Li, Y. Yang, C. Wang, Z. Liu, X. Zhang, F. An, X. Diao, X. Hao, X. Zhang, *Chem. Commun.* 2012, **48**, 8120.
- 24 W. Li, X. Zhang, X. Hao, J. Jie, B. Tian, X. Zhang, *Chem. Commun.* 2013, **49**, 10989.
- 25 P. Huang, D. Wang, Y. Su, W. Huang, Y. Zhou, D. Cui, X. Zhu, D. Yan, *J. Am. Chem. Soc.* 2014, **136**, 11748.
- 26 J. Zhang, Y. Li, F. F. An, X. Zhang, X. Chen, C. S. Lee, *Nano Lett.* 2015, **15**, 313.
- 27 S. Santra, C. Kaitanis, O. J. Santiesteban, J. M. Perez, *J. Am. Chem. Soc.* 2011, **133**, 16680.
- 28 G. Lee, K. Eom, J. Park, J. Yang, S. Haam, Y. Huh, J. K. Ryu, N. H. Kim, J. I. Yook, S. W. Lee, D. S. Yoon, T. Kwon, *Angew. Chem. Int. Ed.* 2012, **51**, 5939.
- 29 J. Lai, B. P. Shah, E. Garfunkel, K. Lee, *ACS Nano* 2013, **7**, 2741.
- 30 Q. Wang, Y. Bao, J. Ahire, Y. Chao, *Adv. Healthcare Mater.* 2013, **2**, 459.
- 31 J. Tang, B. Kong, H. Wu, M. Xu, Y. Wang, Y. Wang, D. Zhao, G. Zheng, *Adv. Mater.* 2013, **25**, 6569.
- 32 Y. Yuan, Y. Chen, B. Z. Tang, B. Liu, *Chem. Commun.* 2014, **50**, 3868.
- 33 Q. Xing, N. Li, D. Chen, W. Sha, Y. Jiao, X. Qi, Q. Xua, J. Lu, *J. Mater. Chem. B* 2014, **2**, 1182.
- 34 M. Zheng, S. Liu, J. Li, D. Qu, H. Zhao, X. Guan, X. Hu, Z. Xie, X. Jing, Z. Sun, *Adv. Mater.* 2014, **26**, 3554.
- 35 Y. Yang, X. Zhang, C. Yu, X. Hao, J. Jie, M. Zhou, X. Zhang, *Adv. Healthcare Mater.* 2014, **3**, 906.
- 36 H. Tang, C. J. Murphy, B. Zhang, Y. Shen, E. A. V. Kirk, W. J. Murdoch, M. Radosz, *Biomaterials* 2010, **31**, 7139.
- 37 S. Barui, S. Saha, G. Mondal, S. Haseena, A. Chaudhuri, *Biomaterials* 2014, **35**, 1643.
- 38 D. Jin, K. W. Park, J. H. Lee, K. Song, J. G. Kim, M. L. Seo, J. H. Jung, *J. Mater. Chem.* 2011, **21**, 3641.
- 39 C. Xu, Y. Niu, A. Popat, S. Jambhrunkar, S. Karmakar, C. Yu, *J. Mater. Chem. B* 2014, **2**, 253.
- 40 S. Dey, K. Sreenivasan, *J. Mater. Chem. B* 2015, **3**, 824.

- 41 H. Wang, S. Zhao, P. Agarwal, J. Dumbleton, J. Yu, X. Lu, X. He, *Chem. Commun.* 2015, **51**, 7733.
- 42 C. Stigliano, J. Key, M. Ramirez, S. Aryal, P. Decuzzi, *Adv. Funct. Mater.* 2015, **25**, 3371.
- 43 J. Zhang, F. An, Y. Li, C. Zheng, Y. Yang, X. Zhang and X. Zhang, *Chem. Commun.* 2013, **49**, 8072.
- 44 C. Yu, M. Zhou, X. Zhang, W. Wei, X. Chen and X. Zhang, *Nanoscale* 2015, **7**, 5683.
- 45 K. Pu, A. J. Shuhendler, J. V. Jokerst, J. Mei, S. S. Gambhir, Z. Bao, J. Rao, *Nat. Nanotechnol.* 2014, **9**, 233.
- 46 A. J. Shuhendler, K. Pu, L. Cui, J. P. Uetrecht, J. Rao, *Nat. Biotech.* 2014, **32**, 373.
- 47 I. C. Wu, J. Yu, F. Ye, Y. Rong, M. E. Gallina, B. S. Fujimoto, Y. Zhang, Y. H. Chan, W. Sun, X.H. Zhou, C. Wu, D. T. Chiu, *J. Am. Chem. Soc.* 2015, **137**, 173.
- 48 G. Prencipe, S. M. Tabakman, K. Welsher, Z. Liu, A. P. Goodwin, L. Zhang, J. Henry, H. Dai, *J. Am. Chem. Soc.* 2009, **131**, 4783.
- 49 K. Fuhrmann, J. D. Schulz, M. A. Gauthier, J. Leroux, *ACS Nano* 2012, **6**, 1667.
- 50 J. Logie, S. C. Owen, C. K. McLaughlin, M. S. Shoichet, *Chem. Mater.* 2014, **26**, 2847.
- 51 H. S. S. Qhattal, T. Hye, A. Alali, X. Liu, *ACS Nano* 2014, **8**, 5423.
- 52 C. Wang, L. Cheng, Z. Liu, *Biomaterials* 2011, **32**, 1110.
- 53 C. Wang, X. X. Ma, S. Q. Ye, L. Cheng, K. Yang, L. Guo, C. H. Li, Y. G. Li, Z. Liu, *Adv. Funct. Mater.* 2012, **22**, 2363.